Synthesis, Preclinical Validation, Dosimetry, and Toxicity of ^{68}Ga-NOTA-Anti-HER2 Nanobodies for iPET Imaging of HER2 Receptor Expression in Cancer

Catarina Xavier[1], Ilse Vaneycken[1,2], Matthias D'huyvetter[1], Johannes Heemskerk[2], Marleen Keyaerts[1,2], Cécile Vincke[3,4], Nick Devoogdt[1,3], Serge Muyldermans[3,4], Tony Lahoutte[1,2], and Vicky Caveliers[1,2]

[1]In Vivo Cellular and Molecular Imaging Laboratory, Vrije Universiteit Brussel, Brussels, Belgium; [2]Nuclear Medicine Department, UZ Brussel, Brussels, Belgium; [3]Laboratory of Cellular and Molecular Immunology, Vrije Universiteit Brussel, Brussels, Belgium; and [4]Department of Structural Biology, VIB, Brussels, Belgium

Nanobodies are the smallest fully functional antigen-binding antibody fragments possessing ideal properties as probes for molecular imaging. In this study we labeled the anti–human epidermal growth factor receptor type 2 (HER2) Nanobody with ^{68}Ga via a 1,4,7-triazacyclononane-1,4,7-triacetic acid (NOTA) derivative and assessed its use for HER2 iPET imaging. **Methods:** The 2Rs15dHis$_6$ Nanobody and the lead optimized current-good-manufacturing-practice grade analog 2Rs15d were conjugated with S-2-(4-isothiocyanatobenzyl)-1,4,7-triazacyclononane-1,4,7-triacetic acid (p-SCN-Bn-NOTA) to enable fast and efficient ^{68}Ga labeling. Biodistribution and PET/CT studies were performed on HER2-positive and -negative tumor xenografts. The effect of injected mass on biodistribution was evaluated. The biodistribution data were extrapolated to calculate radiation dose estimates for the adult female using OLINDA software. A single-dose extended-toxicity study for NOTA-2Rs15d was performed on healthy mice up to a dose of 10 mg/kg. **Results:** Radiolabeling was quantitative (>97%) after 5 min of incubation at room temperature; specific activity was 55–200 MBq/nmol. Biodistribution studies showed fast and specific uptake (percentage injected activity [%IA]) in HER2-positive tumors (3.13 ± 0.06 and 4.34 ± 0.90 %IA/g for ^{68}Ga-NOTA-2Rs15dHis$_6$ and ^{68}Ga-NOTA-2Rs15d, respectively, at 1 h after injection) and high tumor-to-blood and tumor-to-muscle ratios at 1 h after injection, resulting in high-contrast PET/CT images with high specific tumor uptake. A remarkable finding of the biodistribution studies was that kidney uptake was reduced by 60% for the Nanobody lacking the C-terminal His$_6$ tag. The injected mass showed an effect on the general biodistribution: a 100-fold increase in NOTA-2Rs15d mass decreased liver uptake from 7.43 ± 1.89 to 2.90 ± 0.26 %IA/g whereas tumor uptake increased from 2.49 ± 0.68 to 4.23 ± 0.99 %IA/g. The calculated effective dose, based on extrapolation of mouse data, was 0.0218 mSv/MBq, which would yield a radiation dose of 4 mSv to a patient after injection of 185 MBq of ^{68}Ga-NOTA-2Rs15d. In the toxicity study, no adverse effects were observed after injection of a 10 mg/kg dose of NOTA-2Rs15d.

Conclusion: A new anti-HER2 PET tracer, ^{68}Ga-NOTA-2Rs15d, was synthesized via a rapid procedure under mild conditions. Preclinical validation showed high-specific-contrast imaging of HER2-positive tumors with no observed toxicity. ^{68}Ga-NOTA-2Rs15d is ready for first-in-human clinical trials.
Key Words: [68]Ga; Nanobodies; HER2; iPET; NOTA

The human epidermal growth factor receptor type 2 (HER2) is a transmembrane tyrosine kinase that is overexpressed in different types of cancer such as breast (20%–30%), ovarian, prostatic, and colorectal (1). Overexpression of this membrane protein is associated with tumor aggressiveness and an increased probability for recurrent disease, especially in breast cancer patients (1,2). There is a clinical need for accurate determination of the HER2 status of tumors because of its prognostic value and the need for identification of patients who would benefit from targeted anti-HER2 treatment (2,3). Detection of HER2 expression via PET imaging may have important advantages over the current ex vivo tests such as immunohistochemistry and fluorescence in situ hybridization staining of tumor biopsy samples: both primary tumor and metastases can be evaluated by a single noninvasive total-body imaging procedure, sampling errors of biopsies are avoided in the case of HER2 expression heterogeneity, and the procedure is operator-independent and can easily be repeated, thereby avoiding repeated biopsy (3,4). PET imaging might also allow a more accurate quantitative assessment of the total amount of HER2 expression in an individual patient—a quality that could be important for the determination of treatment doses of anti-HER2 therapies. Radionuclide molecular imaging of HER2 overexpression has been performed clinically on breast cancer patients mainly using radiolabeled intact IgG monoclonal antibodies (5,6) and preclinically using antibody fragments such as fragment antigen binding (7),

single-chain variable fragments (8), V_{HH} fragments (Nanobodies, a trade name of Ablynx) (9), diabodies (10), and engineered protein scaffolds such as Affibody molecules (Affibody AB) (11–14) and designed ankyrin repeat proteins that are no longer immunoglobulin-based (15). Monoclonal antibodies have a slow blood clearance, necessitating labeling with long-lived isotopes; patients are scanned only 3–4 d after probe injection and the radiation dose delivered to the patient is high (5,6). Small antibody fragments and protein scaffolds have shorter biologic half-lives, enabling labeling with short-lived isotopes; the radiation dose delivered to the patient is reduced and allows a rapid image acquisition, within a few hours, which is beneficial for the patient (9–15).

Nanobodies are the smallest (12–15 kDa) intact antigen-binding fragments derived from heavy-chain–only antibodies occurring naturally in *Camelidae* (16–19). Their high stability, small size, rapid targeting, fast blood clearance, and easy generation make this technology platform attractive for the generic development of probes for in vivo radio-immunodetection of membrane-associated cancer antigens (9,16–19). Recently, we reported the selection of a lead anti-HER2 Nanobody for molecular imaging of HER2 overexpression (9). This screening was performed with ^{99m}Tc-labeled formats, and the 2Rs15dHis$_6$ Nanobody was selected as the lead compound. The data show that HER2 imaging can be performed as early as 1 h after injection with high tumor-to-muscle and tumor-to-blood ratios, enabling the use of short-lived radioisotopes. In anticipation of the clinical translation of this compound, its format was optimized further. First, the hexahistidine (His$_6$) tag was removed because it might induce immune responses (20,21). Second, the nontagged format was produced in current-good-manufacturing-practice (cGMP) grade. Subsequently, a labeled analog was developed for PET. In accordance with the short biologic half-life of the Nanobody, both ^{68}Ga and ^{18}F are ideal. In this study, we focused on ^{68}Ga-labeled anti-HER2 Nanobodies. ^{68}Ga is an attractive positron-emitting radionuclide because it is cyclotron-independently available via the ^{68}Ge/^{68}Ga generator system. The macrocyclic chelator 1,4,7-triazacyclononane-1,4,7-triacetic acid (NOTA) and its derivatives are particularly interesting for ^{68}Ga complexation because of their fast and efficient radiolabeling at room temperature and high in vivo stability (22,23). The high stability constant of Ga(III)-NOTA complexes (log K_{ML} (stability constant) = 31.0) and their kinetics certainly reflect a better fitting of the NOTA cavity size with the size of the Ga(III) ion and the involvement of all pendant arms in the coordination to the metal (22,23). Both 2Rs15dHis$_6$ and cGMP grade 2Rs15d were conjugated to a S-2-(4-isothiocyanatobenzyl)-1,4,7-triazacyclononane-1,4,7-triacetic acid (p-SCN-Bn-NOTA) derivative and radiolabeled, in view of comparing the 2 formats and validating them preclinically. The aim of the current study was to develop a PET analog of the anti-HER2 Nanobody and measure its specific targeting, biodistribution, dosimetry, and toxicity in animal models in preparation for the first clinical application.

MATERIALS AND METHODS

All commercially obtained chemicals were of analytic grade. p-SCN-Bn-NOTA was purchased from Macrocyclics. ^{68}Ga was obtained from a ^{68}Ge/^{68}Ga generator (Eckert and Ziegler) eluted with 0.1N HCl (Merck). Buffers used for coupling reactions or for radiolabeling were purified from metal contamination using Chelex 100 resin (Aldrich).

Production and Purification of Nanobody

The anti-HER2 Nanobody 2Rs15dHis$_6$ was produced as described previously (9). 2Rs15d was further purified from periplasmic extracts by cation exchange chromatography on CaptoS resin (GE Healthcare) and hydroxyapatite chromatography (Macro Prep Ceramic Hydroxyapatite type I, 40 μm; Bio-Rad), followed by buffer exchange to phosphate-buffered saline (PBS).

Chromatographic Analysis

Size-exclusion chromatography (SEC) was performed on a Superdex 75 10/300 GL column (GE Healthcare) using 0.01 M phosphate buffer and 0.14 M NaCl, pH 7.4, at a flow rate of 0.5 mL min^{-1}. A polystyrene divinylbenzene copolymer column (PLRP-S 30 Å, 5 μm, 250/4 mm; Varian) was used in the case of reverse-phase high-performance liquid chromatography (RP-HPLC) with the following gradient (A: 0.1% trifluoroacetic acid in water; B: acetonitrile): 0–5 min, 25% B; 5–7 min, 25%–34% B; 7–10 min, 75%–100% B; and 10–25 min, 100% B, at a flow rate of 1 mL min^{-1}. Instant thin-layer chromatography (ITLC) was performed on silica gel (SG) (Pall Corp. Life Sciences) using 0.1 M sodium citrate pH 5.0 as the eluent.

Conjugation of p-SCN-Bn-NOTA to Nanobodies

Nanobody 2Rs15dHis$_6$ or 2Rs15d (3 mg) in 0.05 M sodium carbonate buffer, pH 8.7 (1.5 mL), was added to p-SCN-Bn-NOTA (10-fold molar excess) and incubated for 2 h at room temperature. The coupling reaction was quenched by adjusting the pH to 7.0–7.4 using HCl, 1N. The conjugate was then purified by SEC using ammonium acetate, 0.1 M, pH 7.0, as the eluent. The number of chelates per Nanobody was determined by electrospray ionization quadrupole time-of-flight mass spectrometry (ESI-Q-TOF-MS). The concentration of NOTA-Nanobodies was determined spectrophotometrically at 280 nm using the corrected extinction coefficient (ε = 49,440 M^{-1}cm^{-1}).

Synthesis of ^{69,71}Ga-NOTA-Nanobodies

A solution of NOTA-Nanobody (500 μg, 38 nmol) in 400 μL of 0.15 M ammonium acetate, pH 5.0, was incubated with Ga(NO$_3$)$_3$·10H$_2$O (208 nmol) for 2 h at room temperature and purified by ultrafiltration to remove free gallium. ^{69,71}Ga-NOTA-Nanobodies, characterized by ESI-Q-TOF-MS, were used as the reference for the identification of the radio-HPLC/SEC chromatogram signals and to determine the equilibrium dissociation constant.

Preparation of ^{68}Ga-NOTA-Nanobodies

The pH of the peak fraction of the ^{68}Ge/^{68}Ga generator eluate was adjusted to 5 by adding 36 mg of sodium acetate per milliliter of eluate (0.26 M). To 500−1,500 μL of this solution (40–400 MBq), NOTA-Nanobody (1.25–5 nmol) was added and incubated for 5 min at room temperature. Next, the product was purified by gel filtration on a disposable NAP-5 or PD10 column (GE Healthcare). The sample was finally passed through a 0.22-μm membrane filter (4 mm; Millipore), and the final solution was analyzed

by RP-HPLC, SEC, and ITLC-SG (RP-HPLC: retention time $[t_R] = 12.8$ min; SEC: $t_R = 27.6$ min; ITLC-SG: ^{68}Ga-NOTA-Nanobody $R_f = 0$, ^{68}Ga-citrate $R_f = 1$).

Surface Plasmon Resonance

Surface plasmon resonance measurements were performed on a Biacore T200 instrument (GE Healthcare) exactly as described previously (9).

In Vitro Stability of ^{68}Ga-NOTA-Nanobodies

To determine plasma and PBS stability, ^{68}Ga-NOTA-Nanobodies (6–12 MBq) were added to 200 μL of human plasma or 500 μL of PBS and incubated at 37°C for 1 h (and up to 4 h in the case of PBS) and analyzed by SEC and ITLC-SG.

Specificity Experiment with ^{68}Ga-NOTA-Nanobodies

SK-OV-3 and MDA-MB-435D cells were cultured as described previously (9), and the experiment was performed as described previously (9).

Animal Model

To evaluate biodistribution and tumor uptake, female athymic nude mice (5 wk old) and female athymic nude rats (7 wk old) (Harlan) were subcutaneously inoculated in the right hind leg (mice) or in the right shoulder (rats) with either SK-OV-3 (4×10^6 for mice and 15×10^6 for rats) or MDA-MB-435D (1×10^6) cells suspended in PBS, under the control of 2.5% isoflurane in oxygen (Abbott). The tumors were allowed to grow for 1–2 wk to reach 35–100 mm³ in mice and 500–1,000 mm³ in rats. The local ethical committee for animal research approved the animal study protocols.

Ex Vivo Biodistribution Studies

Xenograft tumor–bearing mice were injected intravenously with 2–4 MBq of ^{68}Ga-NOTA-Nanobodies ($n = 5$–6 per compound) (4 μg of NOTA-Nanobody) to evaluate biodistribution at 1 h after injection. To study the influence of injected Nanobody (2Rs15d) mass on the biodistribution profile, the protein quantity was adjusted by dilution of the starting labeling preparation (^{68}Ga-NOTA-2Rs15d) with PBS to provide tracer doses containing 0.1 μg (0.0075 nmol), 1 μg (0.075 nmol), and 10 μg (0.75 nmol) ($n = 6$ for each subgroup). For dosimetry studies, the mice were injected with 5–11 MBq (10 μg of 2Rs15d) and biodistribution was evaluated at 30 min, 1 h, and 3 h after injection ($n = 6$ for each time point). All injections were performed via the tail vein under the control of 2.5% isoflurane in oxygen. The mice were sacrificed, and main organs and tissues were dissected, washed, weighed, and counted against a standard of known activity in a γ-counter. Tissue and organ uptake was calculated and expressed as percentage injected activity (%IA) or %IA per gram, corrected for decay. Additionally, a sample of urine was taken at 1 h after injection and analyzed by SEC.

Radiation dose estimates for the adult female were calculated from the biodistribution data of mice using OLINDA 1.0 software. The calculations were based on time–activity curves to determine the number of disintegrations in 20 source organs. Organ doses, effective dose, and effective dose equivalent were calculated using the appropriate weighting factors for the various organs.

PET/CT Imaging

SK-OV-3 and MDA-MB-435D xenograft rats ($n = 6$) were intravenously injected with 9 MBq of ^{68}Ga-NOTA-2Rs15d (7 μg of NOTA-Nanobody). The rats were anesthetized with a mixture of 75 mg/kg ketamine hydrochloride (Ketamine 1000; CEVA) and 10 mg/kg xylazine hydrochloride (Rompun; Bayer) 45 min after probe administration. The acquisition was performed on a clinical Gemini time-of-flight PET/CT scanner (Philips) at 1 h after injection. The CT acquisition was set to 80 kV at 250 mAs at a resolution of 2 mm, using filtered backprojection for image reconstruction. The total CT scanning time was 20 s. PET images were acquired over 35 min and reconstructed to 234 slices of 288×288 pixels (at a 2-mm isotropic pixel size), with attenuation correction based on the CT data. The images were analyzed using AMIDE. Regions of interest based on the CT image were drawn over the tumors. Background regions of interest were obtained by mirroring the region of interest to the corresponding contralateral muscle area. The ratio between the maximum counts in the tumor region and the maximum counts in the corresponding contralateral region was calculated for all the animals and is referred to as the tumor-to-muscle ratio (mean ± SD).

Toxicity Study with NOTA-2Rs15d

An extended single-dose intravenous toxicity study with NOTA-2Rs15d was performed at TNO Triskelion. The objective of the study was to provide data on the local and systemic toxicity of NOTA-2Rs15d after a single intravenous administration in 6-wk-old female CD-1 mice. The ICH M3 (R2) guideline was applied (guidance on nonclinical safety studies for the conduct of human clinical trials and marketing authorization of pharmaceuticals [CPMP/ICH/286/95]).

RESULTS

Synthesis

p-SCN-Bn-NOTA was conjugated on ε-amino groups of the lysine forming a thiourea bond, represented in Figure 1. The Nanobodies contain 6 lysine residues in the framework regions but none in the complementarity-determining regions (antigen-binding loops). Consequently, the conjugation reaction resulted in a mixture of molecules with 0, 1, 2, and 3 NOTA chelators, as determined by ESI-Q-TOF-MS analysis (Supplemental Fig. 1; supplemental materials are available online at http://jnm.snmjournals.org). The relative protein-to-chelator ratios can be found in Table 1.

HER2 Antigen Binding Characteristics of Chemically Modified Nanobodies

Surface plasmon resonance experiments were performed on immobilized HER2-Fc protein to confirm the affinity of chemically modified Nanobodies toward the protein and to determine binding kinetics parameters (Table 1). All Nanobody derivatives (Nanobody, NOTA-Nanobody, and ^{69,71}Ga-NOTA-Nanobody) bound to the HER2 target protein with affinities in the low-nanomolar range, with no pronounced effect from conjugation of the NOTA chelator or complexation with ^{69,71}Ga (Table 1).

Synthesis, Characterization, and Stability Studies of ^{68}Ga-Labeled Nanobodies

The NOTA-conjugated Nanobodies were labeled at room temperature and pH 5.0 (Fig. 1). The radioactivity incorporation of ^{68}Ga reached more than 97% within 5 min, with a specific activity of 55–200 MBq/nmol. After purification, the compounds were characterized by ITLC-SG, SEC, and RP-HPLC (Figs. 2 and 3), and radiochemical purity was
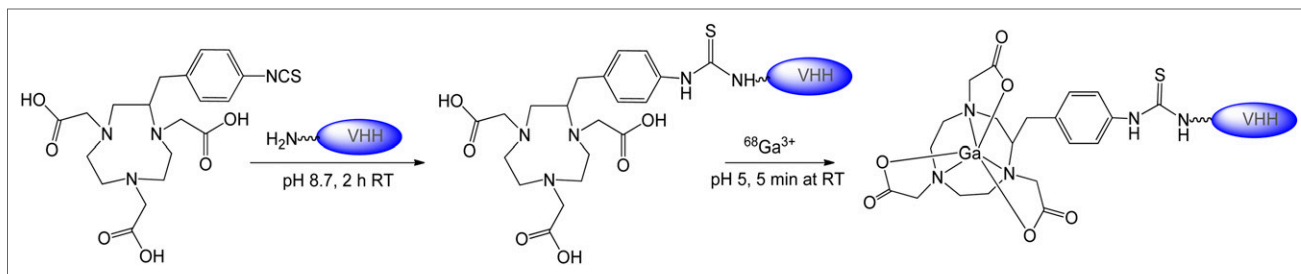
FIGURE 1. Scheme of conjugation reaction of *p*-SCN-Bn-NOTA to Nanobodies and subsequent ^{68}Ga complexation. RT = room temperature.

more than 99%. The chemical identity of the ^{68}Ga complexes was confirmed by comparison of their SEC/RP-HPLC profile with those of the corresponding nonradioactive [69,71]Ga-NOTA Nanobodies (Fig. 2). The radiocompounds proved to be stable in PBS over a 4-h period, with no additional radio-SEC signals (Fig. 2). Incubation of ^{68}Ga-NOTA-Nanobodies in human plasma shows high metabolic stability, as well as high stability with regard to transchelation. After 1 h at 37°C, gel filtration analysis indicated that more than 98% of the activity corresponded to intact radiocompound. After 4 h of incubation at room temperature, ^{68}Ga-labeled compounds were found to be kinetically inert, presenting no degradation or transchelation (Supplemental Table 1).

Cell Binding and Specificity

To assess the functionality and specificity of the ^{68}Ga-NOTA-Nanobodies against the HER2 protein, cell-binding studies on HER2-positive SK-OV-3 cells and HER2-negative MDA-MB-435D cells were performed. To demonstrate that the binding is receptor-specific, a 1,000-fold excess of cold Nanobody was added to HER2-positive cells in the control experiments (Fig. 4). The results showed that the binding of ^{68}Ga-NOTA-Nanobodies was receptor-mediated and could be prevented by receptor saturation. Moreover, the binding of the labeled Nanobodies on HER2-negative cells was negligible and comparable to that of the saturation control experiment (Fig. 4).

Biodistribution Studies

A summary of the biodistribution data for ^{68}Ga-NOTA-2Rs15dHis$_6$ and ^{68}Ga-NOTA-2Rs15d in HER2-positive SK-OV-3 and HER2-negative MDA-MB-435D tumor–bearing mice is presented in Table 2. Measurement of organ radioactivity 1 h after injection showed high kidney retention but low activity in the liver (<1 %IA/g) and remaining organs (≤0.5 %IA/g), except for the HER2-positive tumor. Uptake in the positive tumors was rapid and high, with 3.13 ± 0.06 and 4.34 ± 0.90 %IA/g for ^{68}Ga-NOTA-2Rs15dHis$_6$ and ^{68}Ga-NOTA-2Rs15d, respectively. Uptake in the negative tumor was minor, with values being less than 0.5 %IA/g. Fast washout of radioactivity from the blood and muscle resulted in high tumor-to-muscle and tumor-to-blood ratios at 1 h after injection. The ratios were higher for ^{68}Ga-NOTA-2Rs15d (tumor-to-muscle ratio, 28.49 ± 0.25; tumor-to-blood ratio, 14.11 ± 3.24) than for ^{68}Ga-NOTA-2Rs15dHis$_6$ (tumor-to-muscle ratio, 12.96 ± 2.71; tumor-to-blood ratio, 9.51 ± 2.87). A remarkable difference between the 2 radiocompounds was found for kidney uptake. A decrease of more than 60% was observed for the Nanobody format without the His$_6$ tail at the C terminus (^{68}Ga-NOTA-2Rs15d), demonstrating that the tag had a significant impact on kidney retention. In the urine, only intact ^{68}Ga-NOTA Nanobody was detected (Supplemental Fig. 2), being further evidence of the high in vivo stability of the complexes.

TABLE 1
Surface Plasmon Resonance Results for Nanobodies Binding to Immobilized HER2-Fc Recombinant Protein

Compound	Chelator-to-protein ratio*	k_a (M^{-1}s^{-1})	k_d (s^{-1})	K_D (nM)
2Rs15dHis$_6$	0	$2.27 \pm 0.01 \times 10^5$	$7.02 \pm 0.09 \times 10^{-4}$	3.09 ± 0.04
NOTA-2Rs15dHis$_6$	1.5	$1.12 \pm 0.01 \times 10^5$	$5.64\ 0.14 \times 10^{-4}$	5.05 ± 0.13
[69,71]Ga-NOTA-2Rs15dHis$_6$	1.5	$1.68 \pm 0.01 \times 10^5$	$7.79 \pm 0.11 \times 10^{-4}$	4.64 ± 0.07
2Rs15d	0	$1.95 \pm 0.01 \times 10^5$	$6.12 \pm 0.09 \times 10^{-4}$	3.14 ± 0.05
NOTA-2Rs15d	1.5	$1.41 \pm 0.01 \times 10^5$	$8.72 \pm 0.09 \times 10^{-4}$	4.06 ± 0.07
[69,71]Ga-NOTA-2Rs15d	1.5	$1.84 \pm 0.01 \times 10^5$	$7.20 \pm 0.09 \times 10^{-4}$	3.91 ± 0.05

*Estimation based on ESI-Q-TOF-MS results.
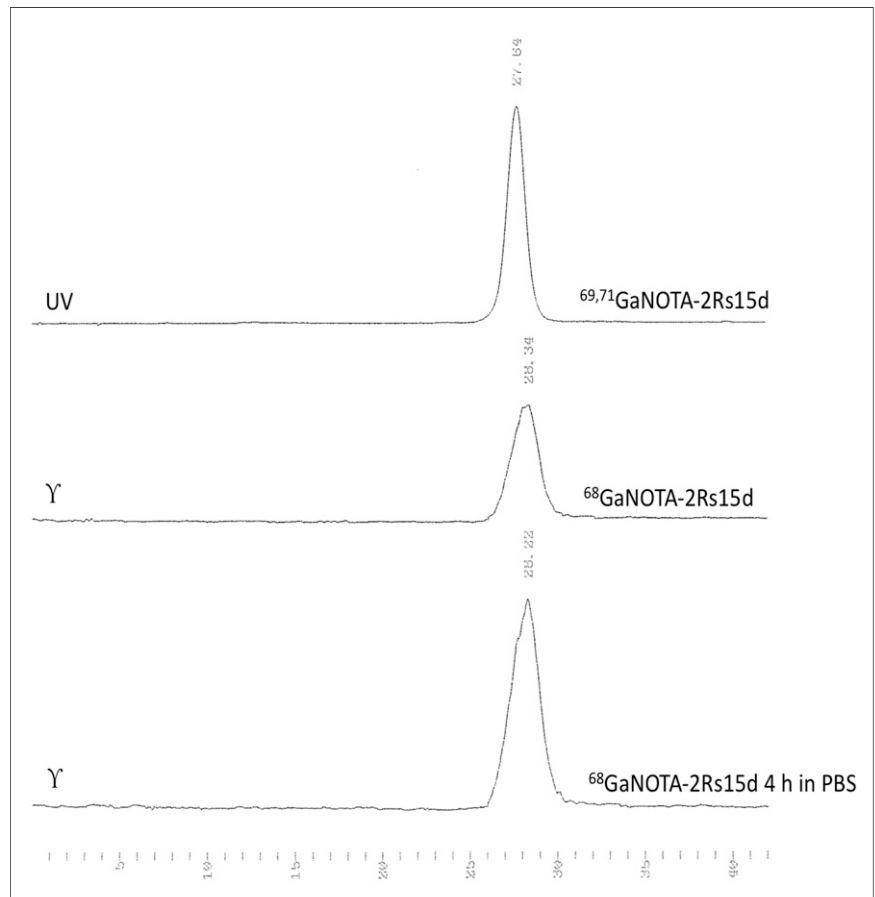k_a = association rate constant; k_d = dissociation rate constant; K_D = equilibrium dissociation constant

FIGURE 2. SEC analysis of ^{69,71}Ga-NOTA-2Rs15d (ultraviolet [UV] absorbance at 280 nm, t_R = 27.64 min) and ^{68}Ga-NOTA-2Rs15d after purification and after 4 h in PBS (radioactive profile, t_R = 28.34 and 28.22 min, respectively).

Influence of Injected NOTA-2Rs15d Mass on Biodistribution Profile of ^{68}Ga-NOTA-2Rs15d

To study the influence of injected tracer mass on uptake in normal tissues and tumor, the biodistribution of ^{68}Ga-NOTA-2Rs15d, containing 3 different quantities of protein, was evaluated at 1 h after injection in HER2-positive SK-OV-3 tumor–bearing mice (Table 3). The accumulation of radioactivity in blood, lungs, spleen, and liver decreased
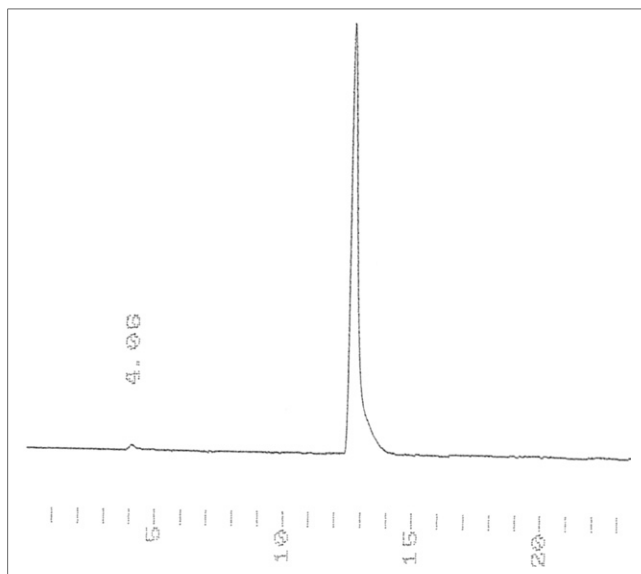

FIGURE 3. RP-HPLC analysis of ^{68}Ga-NOTA-2Rs15d (radioactive profile, t_R = 12.67 min).

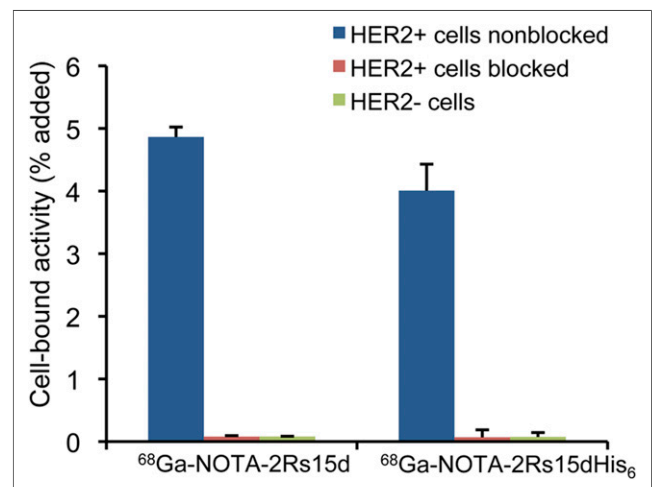**FIGURE 4.** Specificity of ^{68}Ga-NOTA-Nanobodies binding to HER2-positive cells (SK-OV-3) and HER2-negative cells (MDA-MB-435D). HER2 binding was blocked with an excess of Nanobodies (2Rs15dHis$_6$ or 2Rs15d). Binding was specific, as it could be blocked almost completely. Data are presented as mean ± SD (n = 3–4).

TABLE 2
Biodistribution Data of ^{68}Ga-NOTA-Nanobodies at 1 Hour After Injection

| Tissue/organ | ^{68}Ga-NOTA-2Rs15dHis$_6$ | | ^{68}Ga-NOTA-2Rs15d | |
	SK-OV-3	MDA-MB-435D	SK-OV-3	MDA-MB-435D
Lungs	0.52 ± 0.16	0.39 ± 0.10	0.39 ± 0.04	0.39 ± 0.06
Heart	0.14 ± 0.03	0.18 ± 0.01	0.14 ± 0.02	0.17 ± 0.01
Liver	0.75 ± 0.14	0.92 ± 0.09	0.67 ± 0.25	0.78 ± 0.08
Kidney	116.67 ± 1.83	108.02 ± 23.05	45.00 ± 11.42	33.81 ± 6.40
Spleen	0.51 ± 0.06	0.40 ± 0.12	0.28 ± 0.09	0.32 ± 0.07
Muscle	0.25 ± 0.04	0.31 ± 0.27	0.16 ± 0.05	0.16 ± 0.09
Blood	0.35 ± 0.09	0.41 ± 0.01	0.31 ± 0.03	0.46 ± 0.06
Tumor	3.13 ± 0.06	0.45 ± 0.19	4.34 ± 0.90	0.26 ± 0.07
Tumor-to-muscle	12.96 ± 2.71	1.88 ± 1.01	28.49 ± 7.75	1.87 ± 0.85
Tumor-to-blood	9.51 ± 2.87	1.10 ± 0.50	14.11 ± 3.24	0.56 ± 0.14

Data are expressed as mean %IA/g ± SD (n = 5–6). Dose of protein injected (NOTA-2Rs15dHis$_6$ or NOTA-2Rs15d) was 4 μg.

with increasing protein mass (0.1–10 μg), whereas tumor uptake increased (Table 3), resulting in improved tumor-to-organ ratios: the tumor-to-blood ratio increased 3.6-fold, tumor-to-liver 4.1-fold, and tumor-to-muscle 3-fold (Fig. 5).

Dosimetry Analysis

Organ-absorbed doses were estimated by using OLINDA software to extrapolate to the adult female phantom the mouse biodistribution data of ^{68}Ga-NOTA-2Rs15d at different time points. The biodistribution data, which are provided in Supplemental Table 2, were obtained up to 3 h after tracer injection, considered the short half-life of the radionuclide. Table 4 summarizes the organ-absorbed doses. The effective dose was estimated at 0.0218 mSv/MBq; thus, a proposed patient dose of 185 MBq would yield a radiation dose of 4 mSv.

TABLE 3
Influence of Injected 2Rs15d Nanobody Mass on Biodistribution of ^{68}Ga-NOTA-2Rs15d at 1 Hour After Injection

| Tissue/organ | Injected 2Rs15d mass | | |
	0.1 μg	1 μg	10 μg
Blood	1.07 ± 0.24	0.72 ± 0.18	0.50 ± 0.17
Heart	0.53 ± 0.22	0.27 ± 0.05	0.17 ± 0.02
Lungs	8.29 ± 4.89	1.00 ± 0.59	0.53 ± 0.13
Liver	7.43 ± 1.89	3.03 ± 1.00	2.90 ± 0.26
Spleen	2.65 ± 0.89	0.99 ± 0.36	0.71 ± 0.19
Kidney	29.00 ± 3.22	42.90 ± 8.57	38.07 ± 5.69
Intestine	0.38 ± 0.12	0.37 ± 0.20	0.21 ± 0.08
Tumor	2.49 ± 0.68	3.45 ± 1.29	4.23 ± 0.99
Muscle	0.26 ± 0.08	0.24 ± 0.11	0.17 ± 0.15
Tumor-to-muscle	11.09 ± 6.22	15.38 ± 4.82	34.39 ± 15.69
Tumor-to-blood	2.33 ± 0.90	4.92 ± 1.62	8.86 ± 2.61

Data are expressed as mean %IA/g ± SD (n = 6).

PET/CT Imaging

A representative PET/CT whole-body image of a rat bearing an SK-OV-3 tumor and one bearing an MDA-MB-435D tumor at 1 h after injection of ^{68}Ga-NOTA-2Rs15d is shown in Figure 6. High-contrast images were obtained and showed intense tracer uptake in tumors expressing HER2 (SK-OV-3), compared with the nonexpressing tumors (MDA-MB-435D), in which no signal was detected. The tumor-to-muscle ratios were 4.9 ± 0.9 for SK-OV-3 tumors and 1.5 ± 0.3 for MDA-MB-435D tumors. No significant uptake in other organs except for the kidneys and bladder was observed.

Toxicity Study with NOTA-2Rs15d

Overall, no treatment-related toxicologically relevant changes were observed in clinical signs, growth, hematology, clinical chemistry, organ weights, or gross macro- and microscopic observations. Because such changes were absent for up to a 10 mg/kg dose, that dose was considered the no-observed-adverse-effect level for NOTA-2Rs15d in this intravenous extended single-dose toxicity study in female mice.

DISCUSSION

In the present study, ^{68}Ga-labeled anti-HER2 Nanobodies were investigated as potential probes for iPET imaging of HER2 overexpression in cancer. Recently, the selection of the lead compound was reported by our group and was based on a screening of 38 anti-HER2 Nanobodies derived from heavy-chain-only antibodies raised in an immunized dromedary (9). For the screening, Nanobodies were ^{99m}Tc-labeled by site-specifically attaching a ^{99m}Tc-tricarbonyl core at the imidazole residues of the C-terminal histidine tail of the protein. The His$_6$ tag is usually introduced during the Nanobody production to facilitate protein purification. For human applications, however, these so-called fusion proteins with histidine-rich affinity tags are not recommended because of increased risk for immunogenicity (20,21). For this reason, the lead Nanobody 2Rs15d
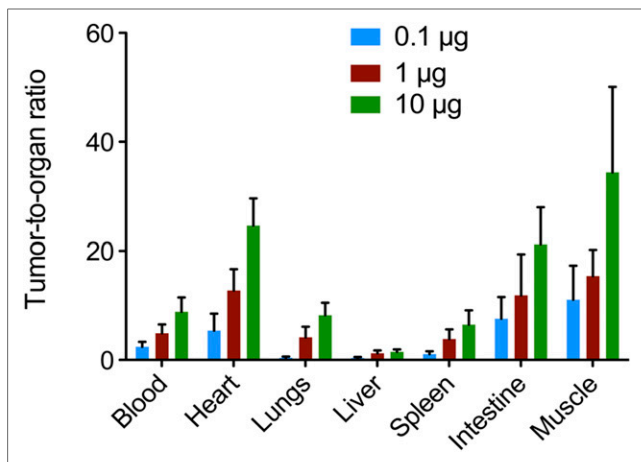
FIGURE 5. Tumor-to-organ ratios for ^{68}Ga-NOTA-2Rs15d in *nu/nu* mice bearing SK-OV-3 xenografts (HER2-positive), at 1 h after injection. Values are presented as mean value ± SD (*n* = 6).
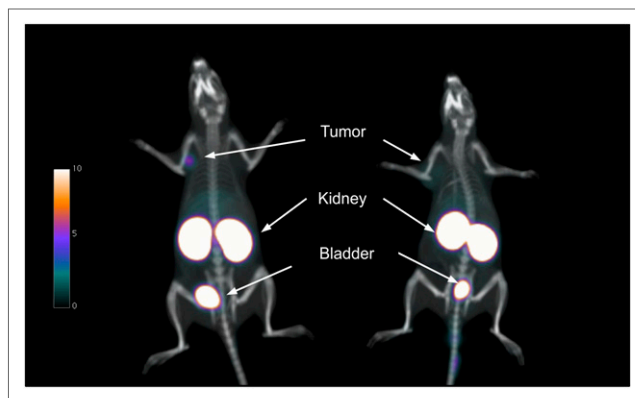

FIGURE 6. PET/CT images of *nu/nu* female rats bearing SK-OV-3 (HER2-positive) (left) or MDA-MB-435D (HER2-negative) (right) tumor xenografts at 1 h after injection of ^{68}Ga-NOTA-2Rs15d.

was produced under cGMP conditions without an His[6] tag. Here, we investigated ^{68}Ga labeling and subsequent in vitro and in vivo evaluation of both the 2Rs15dHis[6] and nontagged 2Rs15d. The *p*-SCN-Bn-NOTA was conjugated to the protein, and radiolabeling with ^{68}Ga was fast and efficient at room temperature. The revealed integrity in physiologic media and human

TABLE 4
Radiation Dose Estimates to Different Organs for Adult Female Human Based on OLINDA Calculations

Target organ	Total (mSv/MBq)
Adrenals	1.24E−02
Brain	1.93E−04
Breasts	5.17E−04
Gallbladder wall	7.92E−03
Lower large intestine wall	7.40E−04
Small intestine	2.71E−03
Stomach wall	2.75E−03
Upper large intestine wall	2.62E−03
Heart wall	3.48E−03
Kidneys	5.92E−01
Liver	2.72E−02
Lungs	3.21E−03
Muscle	1.33E−03
Ovaries	2.12E−02
Pancreas	5.96E−03
Red marrow	2.12E−03
Osteogenic cells	1.20E−03
Skin	6.20E−04
Spleen	1.60E−02
Thymus	3.89E−03
Thyroid	1.98E−03
Urinary bladder wall	4.89E−04
Uterus	1.22E−02
Total body	4.91E−03

Effective dose equivalent (mSv/MBq) = 4.57E−02. Effective dose (mSv/MBq) = 2.18E−02.

plasma confirms high stability of the complexes. We further showed that the nanomolar affinities of neither Nanobody format was affected by chelator conjugation and [69,71]Ga complexation. High specific tumor uptake was observed in biodistribution and PET imaging experiments in nude mice and nude rats bearing HER2-expressing SK-OV-3 xenografts. Tumor uptake of ^{68}Ga-NOTA-2Rs15d was comparable to that of the [99m]Tc(CO)[3]-2Rs15dHis[6] complex (>4 %IA/g), with similar tumor-to-blood ratios (~15) (*9*). The kidney uptake of the ^{99m}Tc complex (154.7 ± 17.7 %IA/g) is higher than that of the ^{68}Ga complex (116.67 ± 1.83 %IA/g) for the same Nanobody format (with histidine tag), being evidently an effect of the radionuclide labeling on kidney retention. Labeling of Nanobodies with ^{68}Ga was reported only by Vosjan et al. (*17*). In that study, an anti–epidermal growth factor receptor Nanobody was labeled with ^{68}Ga using the bifunctional chelator *p*-isothiocyanatobenzyl-desferrioxamine. The achieved radiolabeling yields were lower in their case, at 55%–70%, than the 97% yield in our case, probably because of the lower protein substitution (0.2 chelators per protein vs. 1.5 in our study). The ^{68}Ga-anti–epidermal growth factor receptor Nanobody ([68]Ga-7D12) showed higher tumor uptake at 1 h after injection (6.1 ± 1.3 %IA/g) but lower tumor-to-blood ratios (8 vs. 14) than were obtained with ^{68}Ga-NOTA-2Rs15d (*17*). ^{68}Ga-NOTA-2Rs15d allowed high-contrast imaging at early time points (1 h after injection), in comparison with radiolabeled intact mAbs and antibody fragments used in preclinical or clinical imaging studies (*5–7,24*). In recent studies with [89]Zr-labeled trastuzumab, tumors could be visualized only at 6–24 h after injection, and even then tumor-to-blood ratios reached only approximately 1 after 24 h after injection, and the optimal time point for imaging was only 4–6 d after injection (*6,24*). Although presenting lower absolute tumor uptake than monoclonal antibodies, Nanobodies are more favorable for patient comfort and fast diagnosis. Smaller fragments of the monoclonal antibody trastuzumab, F(ab′)[2] fragments, have also been labeled with ^{68}Ga using the bifunctional

chelator DOTA (7). ^{68}Ga-trastuzumab F(ab')$_2$ fragments presented high tumor uptake of 12 %IA/g at 3.5 h after injection (BT-474 human breast cancer xenografts), but also low tumor-to-blood ratios (<1) were obtained. Affibody molecules have also been labeled with ^{68}Ga for anti-HER2 imaging using the DOTA chelator (13,14,25) and, in a recent publication, the NOTA chelator (11). In these studies, tumor uptake varied from 4.04 ± 0.24 %IA/g at 1 h after injection (14), 5.6 ± 1.6 %IA/g at 1 h after injection (25), and 8.9 %IA/g at 45 min after injection (13) to a remarkable high value of 31 ± 2.1 %IA/g at 1 h after injection (25). In the latter study, the higher tumor uptake might have been due to the fact that the experiment was performed on a different tumor model (BT474 tumors, expressing 3 times higher levels of HER2 than do SK-OV-3 tumors) (3), and a direct comparison cannot be performed. Except for that study (25), the tumor-to-blood ratios at early time points (≤1 h after injection) were lower (5.32 ± 0.18 (14), 6 ± 0.8 (13), and 8.0 ± 1.3 (25)) than the value obtained for ^{68}Ga-NOTA-2Rs15d (14.11 ± 3.24). Kidney uptake in these cases was also high, varying between 146 and 280 %IA/g at 1 h after injection (11,13,14,25).

The most remarkable finding of the biodistribution study with ^{68}Ga-NOTA-anti-HER2 Nanobodies was the much lower retention of activity in the kidneys after removal of the histidine tag. Until now, Nanobodies have always presented intense accumulation in the proximal tubuli of the kidney cortex by a mechanism that is at least partially mediated by the megalin-receptor system (26). The kidney activity could be successfully reduced by coinjection of the Nanobodies with positively charged amino acids and gelofusin, which compete for the renal reabsorption mechanism, an approach that is commonly used for radiolabeled peptide imaging and therapy (27). The observation that the removal of the His$_6$ results in much lower kidney retention could be explained by differences in the overall charge of the Nanobodies because the pH in the kidney is below the pK$_a$ (negative logarithm of the acid ionization constant) of the imidazol groups. Presumably, other factors besides charge effects also are involved in the mechanism of kidney retention, and it is important to address this issue especially with regard to therapeutic applications of Nanobodies radiolabeled with β$^-$-emitting radionuclides (28).

The injected protein mass (2Rs15d) has an important effect on the uptake of ^{68}Ga-NOTA-2Rs15d in normal organs and tumor. We hypothesize that, because of the fast clearance of the tracer, a certain mass of Nanobody is needed to block nonspecific uptake of the ^{68}Ga-NOTA-2Rs15d probe in normal organs (lungs, spleen, liver). Increasing the mass of cold protein from 0.1 to 10 μg makes more available for diffusion to the high-affinity tumor sites, leading to increased specific uptake of the radioactive probe and decreased uptake in normal organs. Alternatively, an increased protein mass may induce internalization of the compound and in this way be responsible for enhanced uptake in the tumor. The effect of injected tracer mass on the biodistribution pattern will be further addressed in the clinical trial with ^{68}Ga-NOTA-2Rs15d and also in concomitant experiments with Nanobodies for radionuclide therapy applications. The ideal mass is the one for which we see tumor targeting at an intensity of accumulation that exceeds the level of accumulation in the liver. This quality is important because the liver is a prime location for metastatic HER2-positive cancer lesions. To our knowledge, this report is also the first of toxicity results with a NOTA-derivatized compound, for which no adverse effects were observed after injection of a 10 mg/kg dose of NOTA-2Rs15d. In addition, we also show for the first time extrapolated dosimetry results for a Nanobody-derivatized tracer. The estimated radiation dose is lower for ^{68}Ga-NOTA-2Rs15d (4 mSv for 185 MBq of administered activity) than for a standard ^{18}F-FDG PET scan (7 mSv for 370 MBq of administered activity) and much lower than for an ^{89}Zr-antibody PET scan (40 mSv for 74 MBq of administered activity) (29,30). However, dosimetry data may change with the concentration of injected protein.

Taken together, these data indicate that the reported ^{68}Ga-NOTA-2Rs15d can be regarded as safe for clinical diagnostic translation.

The chemistry and radiochemistry procedures described in this paper are also applicable to other Nanobodies generated against a variety of in vivo molecular targets (16,31,32) and may therefore lead to the generation of a diversity of new PET radiopharmaceuticals. Moreover, the chelator-conjugated Nanobodies might be synthesized in advance and presented as radiopharmaceutical kits. With the rising availability of the ^{68}Ge/^{68}Ga generator worldwide and the fast ^{68}Ga-labeling procedure described here, without the need for time-consuming HPLC purification, this might be an opportunity to easily produce in-house PET tracers in a hospital radiopharmacy setting.

CONCLUSION

A new anti-HER2 iPET tracer, ^{68}Ga-NOTA-2Rs15d, was developed on the basis of Nanobody technology in combination with radiometal chemistry using the short-lived radioisotope ^{68}Ga. Radiolabeling was fast and stable, and the probe showed specific accumulation in xenografts in ex vivo biodistribution studies and in PET/CT imaging. Removal of the histidine tag considerably reduced kidney retention of the Nanobody. This tracer proved to be safe on the basis of mouse toxicity and dosimetry studies. ^{68}Ga-NOTA-2Rs15d is ready for clinical iPET imaging of HER2 receptor expression.

DISCLOSURE

REFERENCES

1. Mendelsohn J, Howley PM, Israel MA, Gray JW, Thompson CB. *The Molecular Basis of Cancer*. Philadelphia, PA: Saunders, Elsevier; 2008:160–161, 339, 425, 427–428, 575.
2. Hicks DG, Kulkarni S. HER2+ breast cancer: review of biologic relevance and optimal use of diagnostic tools. *Am J Clin Pathol*. 2008;129:263–273.
3. Tolmachev V. Imaging of HER-2 overexpression in tumors for guiding therapy. *Curr Pharm Des*. 2008;14:2999–3019.
4. Oude Munnink TH, Nagengast WB, Brouwers AH, et al. Molecular imaging of breast cancer. *Breast*. 2009;18(suppl 3):S66–S73.
5. Perik PJ, Lub-De Hooge MN, Gietema JA, et al. Indium-111-labeled trastuzumab scintigraphy in patients with human epidermal growth factor receptor 2-positive metastatic breast cancer. *J Clin Oncol*. 2006;24:2276–2282.
6. Dijkers EC, Oude Munnink TH, Kosterink JG, et al. Biodistribution of ^{89}Zr-trastuzumab and PET imaging of HER2-positive lesions in patients with metastatic breast cancer. *Clin Pharmacol Ther*. 2010;87:586–592.
7. Smith-Jones PM, Solit DB, Akhurst T, Afroze F, Rosen N, Larson SM. Imaging the pharmacodynamics of HER2 degradation in response to Hsp90 inhibitors. *Nat Biotechnol*. 2004;22:701–706.
8. Adams GP, Schier R, Marshall K, et al. Increased affinity leads to improved selective tumor delivery of single-chain Fv antibodies. *Cancer Res*. 1998;58:485–490.
9. Vaneycken I, Devoogdt N, Van Gassen N, et al. Preclinical screening of anti-HER2 Nanobodies for molecular imaging of breast cancer. *FASEB J*. 2011;25:2433–2446.
10. Olafsen T, Sirk SJ, Olma S, Shen CK, Wu AM. ImmunoPET using engineered antibody fragments: fluorine-18 labeled diabodies for same-day imaging. *Tumour Biol*. 2012;33:669–677.
11. Heskamp S, Laverman P, Rosik D, et al. Imaging of human epidermal growth factor receptor type 2 expression with ^{18}F-labeled affibody molecule $Z_{HER2:2395}$ in a mouse model for ovarian cancer. *J Nucl Med*. 2012;53:146–153.
12. Baum RP, Prasad V, Müller D, et al. Molecular imaging of HER2-expressing malignant tumors in breast cancer patients using synthetic ^{111}In- or ^{68}Ga-labeled affibody molecules. *J Nucl Med*. 2010;51:892–897.
13. Tolmachev V, Velikyan I, Sandstrom M, Orlova AA. HER2-binding Affibody molecule labeled with ^{68}Ga for PET imaging: direct in vivo comparison with the ^{111}In-labelled analogue. *Eur J Nucl Med Mol Imaging*. 2010;37:1356–1367.
14. Ren G, Zhang R, Liu Z, et al. A 2-helix small protein labeled with ^{68}Ga for PET imaging of HER2 expression. *J Nucl Med*. 2009;50:1492–1499.
15. Zahnd C, Kawe M, Stumpp MT, et al. Efficient tumor targeting with high-affinity designed ankyrin repeat proteins: effects of affinity and molecular size. *Cancer Res*. 2010;70:1595–1605.
16. Gainkam LOT, Huang L, Caveliers V, et al. Comparison of the biodistribution and tumor targeting of two ^{99m}Tc-labeled anti-EGFR Nanobodies in mice, using pinhole SPECT/microCT. *J Nucl Med*. 2008;49:788–795.
17. Vosjan MJ, Perk LR, Roovers RC, et al. Facile labelling of an anti-epidermal growth factor receptor Nanobody with ^{68}Ga via a novel bifunctional desferal chelate for immuno-PET. *Eur J Nucl Med Mol Imaging*. 2011;38:753–763.
18. Hamers-Casterman C, Atarhouch T, Muyldermans S, et al. Naturally occurring antibodies devoid of light chains. *Nature*. 1993;363:446–448.
19. Muyldermans S. Single domain camel antibodies: current status. *J Biotechnol*. 2001;74:277–302.
20. Arnau J, Lauritzen C, Petersen GE, Pedersen J. Current strategies for the use of affinity tags and tag removal for the purification of recombinant proteins. *Protein Expr Purif*. 2006;48:1–13.
21. Shimp RL Jr, Martin LB, Zhang Y, et al. Production and characterization of clinical grade Escherichia coli derived Plasmodium falciparum 42kDa merozoite surface protein 1 ($MSP1_{42}$) in the absence of an affinity tag. *Protein Expr Purif*. 2006;50:58–67.
22. Fani M, Andre JP, Maecke HR. ^{68}Ga-PET: a powerful generator-based alternative to cyclotron-based PET radiopharmaceuticals. *Contrast Media Mol Imaging*. 2008;3:67–77.
23. Wadas TJ, Wong EH, Weisman GR, Anderson CJ. Coordinating radiometals of copper, gallium, indium, yttrium, and zirconium for PET and SPECT imaging of disease. *Chem Rev*. 2010;110:2858–2902.
24. Dijkers ECF, Kosterink JGW, Rademaker AP, et al. Development and characterization of clinical grade ^{89}Zr-trastuzumab for HER2/neu immunoPET imaging. *J Nucl Med*. 2009;50:974–981.
25. Kramer-Marek G, Shenoy N, Seidel J, Griffiths GL, Choyke P, Capala J. ^{68}Ga-DOTA-Affibody molecule for in vivo assessment of HER2/neu expression with PET. *Eur J Nucl Med Mol Imaging*. 2011;38:1967–1976.
26. Gainkam LO, Caveliers V, Devoogdt N, et al. Localization, mechanism and reduction of renal retention of technetium-99m labeled epidermal growth factor receptor-specific Nanobody in mice. *Contrast Media Mol Imaging*. 2011;6:85–92.
27. Vegt E, de Jong M, Wetzels JF, et al. Renal toxicity of radiolabeled peptides and antibody fragments: mechanisms, impact on radionuclide therapy, and strategies for prevention. *J Nucl Med*. 2010;51:1049–1058.
28. D'Huyvetter M, Aerts A, Xavier C, et al. Development of ^{177}Lu-Nanobodies for radioimmunotherapy of HER2-positive breast cancer: evaluation of different bifunctional chelators. *Contrast Media Mol Imaging*. 2012;7:254–264.
29. Börjesson PKE, Jauw YWS, de Bree R, et al. Radiation dosimetry of ^{89}Zr-labeled chimeric monoclonal antibody U36 as used for immuno-PET in head and neck cancer patients. *J Nucl Med*. 2009;50:1828–1836.
30. Brix G, Lechel U, Glatting G, et al. Radiation exposure of patients undergoing whole-body dual-modality ^{18}F-FDG PET/CT examinations. *J Nucl Med*. 2005;46:608–613.
31. Broisat A, Hernot S, Toczek J, et al. Nanobodies targeting mouse/human VCAM1 for the nuclear imaging of atherosclerotic lesions. *Circ Res*. 2012;110:927–937.
32. Movahedi K, Schoonooghe S, Laoui D, et al. Nanobody-based targeting of the macrophage mannose receptor for effective in vivo imaging of tumor-associated macrophages. *Cancer Res*. 2012;72:4165–4177.